Fermi National Accelerator Laboratory

FERMILAB-Pub-81/34-EXP
7850.507-II

RADIATION FROM THE CHANNELING OF 10 GeV POSITRONS BY SILICON SINGLE CRYSTALS

N. A. Filatova, V. M. Golovatyuk, A. N. Iskakov,
I. M. Ivanchenko, R. B. Kadyrov, N. N. Karpenko, T. S. Nigmanov,
V. V. Palcnik, V. D. Riabtsov, M. D. Shafranov, E. N. Tsyganov,
I. A. Tyapkin and D. V. Uralski
Joint Institute for Nuclear Research
Dubna, USSR

A. Forycki, Z. Guzik, and J. Wojtkowska
Institute for Nuclear Research
Swierk, Poland

R. A. Carrigan, Jr. and T. E. Toohig
Fermi National Accelerator Laboratory
Batavia, Illinois USA

C. Carmack, W. M. Gibson, I.-J. Kim, and C.-R. Sun
State University of New York at Albany
Albany, New York USA

M. D. Bavizhev, N. K. Bulgakov, and N. I. Zimin
Tomsk Polytechnical Institute
Tomsk, USSR

I. A. Grishaev, G. D. Kovalenko, and B. I. Shramenko
Kharkov Physical-Technical Institute
Kharkov, USSR

E. I. Denisov and V. I. Glebov
Kurchatov Institute of Atomic Energy
Moscow, USSR

and

V. V. Avdeichikov
V. G. Khlopin Radiation Institute
Leningrad, USSR

April 1981

ABSTRACT

An investigation has been carried out of the radiation emitted by 10 GeV positrons planar channeled in perfect single crystals of silicon. The radiation is found to be narrowly peaked in direction and energy as compared with normal bremsstrahlung radiation, consistent with theoretical predictions. Strong evidence is found for structure not resolved in previous experiments, particularly at angles near the critical angle for channeling where the radiation exhibits a marked periodic structure.

Recently it has been demonstrated that the very strong fields inside a perfect single crystal are capable of bending beams of channeled relativistic particles(1). The coherent action of the strong fields within such a perfect crystal is equivalent in bending power to magnetic fields of several megagauss. The investigation of the action of such strong coherent fields on channeled relativistic particles has now been extended to study the radiation due to the coherent action of the scattering centers in perfect single crystals of silicon on channeled positrons with an energy of 10 GeV.

Kumakhov(2) has predicted a type of radiation due to channeling which is specifically different from ordinary bremsstrahlung, coherent bremsstrahlung and transition radiation. This radiation has been detected by experiments performed by a Yerevan-SLAC collaboration(3) a Livermore-Stanford group(4) and a group at Aarhus University(5). This experiment extends those investigations to show evidence for detailed structure in channeling radiation spectra for positrons at high energy.

In order to investigate the radiation due to channeling the apparatus used to establish the bending of the trajectories of channeled particles by perfect single crystals was moved from the extracted proton beam at the 10 GeV Dubna Synchrophasotron to an electron/positron beam at the 76 GeV IHEP accelerator at Serpukhov. The apparatus was redesigned to include a Cesium Iodide spectrometer for photon identification and measurement, and a secondary particle spectrometer for electron/ positron identification and measurement. The revised experimental layout is shown in Figure 1.

Sources of background radiation were eliminated as far as possible by minimizing the amount of radiating material in the beam and introducing of weak magnets to separate upstream photon background sources. Photon sources were removed from the positron beam path with the small steering magnets M1 and M2, which adjusted the positron trajectory upstream and downstream of the target crystal such that background photons produced in the apparatus other than in the crystal or the second drift module passed outside the aperture of the photon spectrometer. Drift chamber module DC2 is a low pressure (150 Torr), low mass chamber contributing only 6×10^{-4} of a radiation length to the background radiation. The region from upstream of M1 to downstream of M2, is under vacuum except for DC2 itself.

The beam is derived from a modified targeting system in the internal beam of the IHEP accelerator. Photons from pi-zero decay emerging at an angle of 2.5 degrees to the circulating beam are converted by a radiator placed outside the accelerator. The measured hadron contamination in the beam is less than 0.5%. The positron beam intensity is 10^5 per 10^{12} protons on the production target.

For the experiment reported here scintillation counters S1, S2, S3, and veto counters A1, A2, A3 formed the event trigger. Drift chamber modules DC1, DC3, and DC4, each consisting of 4 X- and 4 Y-planes, and DC2, consisting of 2 X- and 2-Y planes, were used to record the position coordinates of the positron. Positron identification was provided by the lead glass Cerenkov counter array. The momentum of the positron is measured using the analysing magnet M3. The energy of photons originating in the crystal was measured in the CsI photon spectrometer. The CsI was protected by a lead shield and surrounded by anti-counters A4-A12. Anti-counters A4 and A12 were also used to form a muon trigger for continual calibration of the CsI. The CsI detector consisted of a cylindrical crystal with a diameter of 150mm and a length of 230mm, approximately 13 radiation lengths. The spectrometer was calibrated with Cs, Co, and Po-Be sources. The resolution of the detector, obtained by unfolding the calibration spectra, is around 3% in the region of 1 MeV and approximately 1% in the region of 100 MeV. The most probable energy loss of minimum-ionizing muons was calibrated against the radiation sources. Calibration of the detector was maintained during the experiment by making each 10th trigger a muon trigger.

The silicon single crystal used in the experiment was a disc of approximately 22mm diameter and 0.5mm thickness. A circular section of 18mm was etched to a thickness of 90 microns. A guard ring of solid state counters was mounted with the crystal in the goniometer. The guard ring which had a clear aperture of 22mm, was used to center the crystal in the beam. The crystal was cut normal to the <111> axis within 0.2 degrees. It was pre-aligned by reflecting laser light from the polished surface. The axis was then determined relative to the beam direction by rotating the crystal in the goniometer to find the peak in the number of gamma counts. For the measurements reported here the <111> axis was oriented 0.5 degrees horizontally relative to the beam direction, to eliminate axial channeling while the (110) plane was horizontal and aligned to the beam direction.

All events were recorded which produced a photon of energy greater than 5 MeV in the CsI detector and a positron signal in the lead glass array. To eliminate events due to the low energy tail of the incident positron beam, the minimum energy of the positron as determined by the analysis magnet, M3, was required to be greater than 8 GeV. For each event the incident angle relative to the (110) plane, the photon energy and the secondary positron energy were determined.

Figure 2 presents the spectral density of the radiation as a function of the photon energy for all events lying within 20 microradians of the (110) plane. A line consistent with the apparatus resolution has been fitted through the data to guide the eye. For 10 GeV positrons in silicon the critical angle for channeling in the (110) plane is 65 microradians so the events in Figure 2 are well within the channeling regime. Superimposed on the experimental distribution is a theoretical prediction using the Kumakhov approach. In addition a curve is included that has been fitted through the 10 GeV data on diamond from the Yerevan-SLAC experiment with the energy axis properly scaled to transform from diamond to silicon. The bremsstrahlung spectrum for an amorphous aluminum radiator is also shown. The radiation length for aluminum is only about 1% different from the silicon radiation length.

The data are in reasonable agreement with the channeling prediction: specifically, the radiation due to channeling is of the order of fifty times more intense than ordinary bremsstrahlung radiation, much more narrowly peaked in energy, and the energy of the principal peak near 50 MeV corresponds closely to the Kumakhov prediction. This energy is calculated on the basis of the full Kumakhov theory using the non-dipole calculation necessary at extremely relativistic energies. The absolute rate also agrees with the theory.

Below 50 MeV the data reported here is distinctly different from both the Kumakhov theory and the Yerevan-SLAC data. There is evidence for a narrow, statistically significant peak in the spectral energy distribution in the vicinity of 25 MeV.

The dependence of the radiation intensity on the incident direction of the positrons relative to the (110) plane is plotted in Figures 3a, b, c. Figure 3a shows the angular dependence for all events detected in the photon spectrometer. The distribution is seen to be on the order of 1000 microradians corresponding to the angular acceptance of the apparatus. Figure 3b presents the angular distribution for those positrons producing a photon in the region of the prominent peak of Figure 2, $30<E<80$ MeV. the distribution has a width $\sigma=65$ microradians, comparable to the critical angle and centered about the (110) plane. The flat distribution in Figure 3b may be a hint that excitation at very small angles is suppressed. In any event it is evident that events in the peak of the photon spectrun are strongly correlated with positrons incident within the critical angle for channeling.

Figure 3c shows the incident angular distribution for events with $600 \leqslant E \leqslant 1000$ MeV, well away from the peak of Figure 2. These events are seen to be correlated with positrons incident at angles larger than the critical angle. These photons are consistent with bremsstrahlung production. Bremsstrahlung is strongly reduced for particles in the channeling regime because the particles do not pass close to nuclear centers.

At ultra relativistic energies higher harmonics are generated, particularly for trajectories near the critical angle[6]. Such events appear to give rise to a qualitative difference in the spectral energy distribution between Figures 4a and 4b. Figure 4a does not include the critical angle, while Figure 4b does include the region near the critical angle. Lines consistent with the apparatus resolution are fitted through the data to guide the eye. Although the statistical uncertainty precludes detailed examination, the apparent periodic structure is consistent with the harmonic structure predicted by Kumakhov[6]. It should be noted that this structure is qualitatively different from the spectral structure observed at lower energies in the Livermore[4] and Aarhus[5] studies which were attributed to transitions between discrete bound states for the channeled positrons or electrons. At very high energies, as in the present case the density of states in the potential becomes so high that observation of transitions between discrete levels is precluded.

Further studies are underway to investigate these effects and to get more information on the origin of the sharp peak at 25 MeV.

We would like to thank N.N. Bogolubov and L. Lederman for strong support and encouragement in carrying out this experiment. In addition we would like to thank A.A. Logunov and the staff of the IHEP accelerator for their efforts and support especially in the design of the electron/positron beam channel. We would also like to thank A.M. Baldin and the staff of the Laboratory for High Energies at Dubna for continued support. The U.S. members of the experiment would like to thank the staff of the Joint Institute for Nuclear Research at Dubna for extended hospitality during the course of the experiment.

References

1. A.F. Elishev, N.A. Filatova, V.M. Golovatyuk et al. Phys. Letters, 88B, 387 (1979); Pisma v JETP (USSR), 30, 442 (1979) 43 , 1723 (1979)
2. M.A. Kumakhov, Phys. Letters, 57A, 17 (1976); Zh. Eksper. Teor. Fiz. (JETP,USSR), 72, 1489 (1977)
3. I.I. Miroshnichenko, D.D. Murray, R.O. Avakyan, T.Kh. Fieguth, Pisma v JETP (USSR), 29, 786 (1979)
4. M.J. Alguard, R.L. Swent, R.N. Pantell, B.L. Berman, S.D. Bloom, and S. Datz, Phys. Rev. Letters 42, 1148 (1979);
5. J.U. Andersen and E. Laegsgaard, Phys. Rev. Letters 44, 1079 (80).
6. See for instance R. Wedell, Phys. Stat. Sol. (b) 99, 11 (1980). This article contains a complete review of earlier work on channeling radiation.

<u>Figure 1</u> Experimental apparatus. S1-4 are the trigger counters while A1-12 are the vetoes. DC1-4 are drift chambers modules. M, M1-3 are magnets for calibration and background elimination. C1 and C2 are threshold Cherenkov counters.

<u>Figure 2</u> Spectral density of channeling radiation due to positrons incident on the silicon crystal in angular range $0 \leq \theta \leq 20$ microradians, well within the critical angle. The solid line is a curve consistent with the resolution placed through the experimental data to guide the eye. The dashed line is a theoretical calculation. The dotted line represents the Yerevan-SLAC data on diamond renormalized to silicon. Points are measurements of ordinary bremsstahlung on an amorphous aluminum sample.

<u>Figure 3</u> Incident angular distribution for positrons:

a. within the aperture of the spectrometer

b. producing a photon in the peak region $30 \leq E \leq 80$ MeV for channeling radiation

c. producing a photon in the range $600 \leq E \leq 1000$ MeV corresponding to typical bremsstrahlung energies.
(Note that the range of angles differs for each curve.)

<u>Figure 4</u> Spectral density distribution for photons produced by positrons whose incident angles:

a. lie inside the critical angle

b. includes the region near the critical angle
(solid lines are curves to guide the eye.)

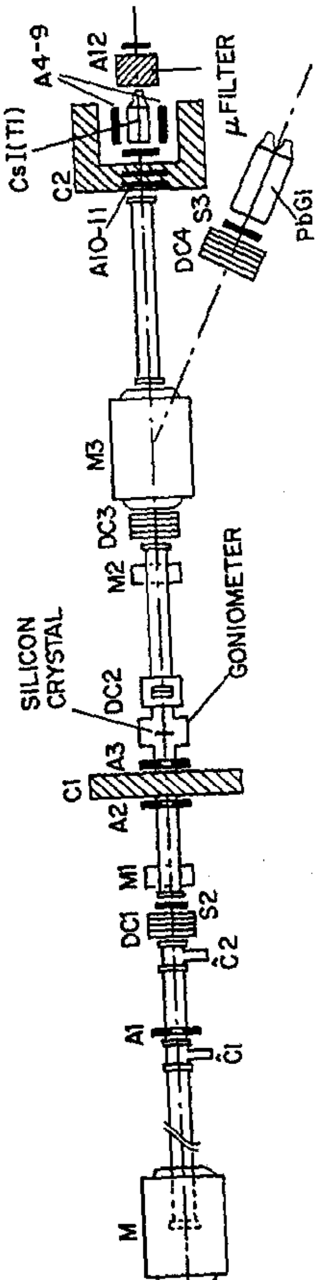

S1
M
A1
Ĉ1
Ĉ2
DC1
S2
M1
A2
C1
A3
SILICON
CRYSTAL
DC2
GONIOMETER
M2
DC3
M3
A10-11
DC4
S3
PbGl
C2
CsI(Tl)
A4-9
A12
μFILTER

Fig. 1

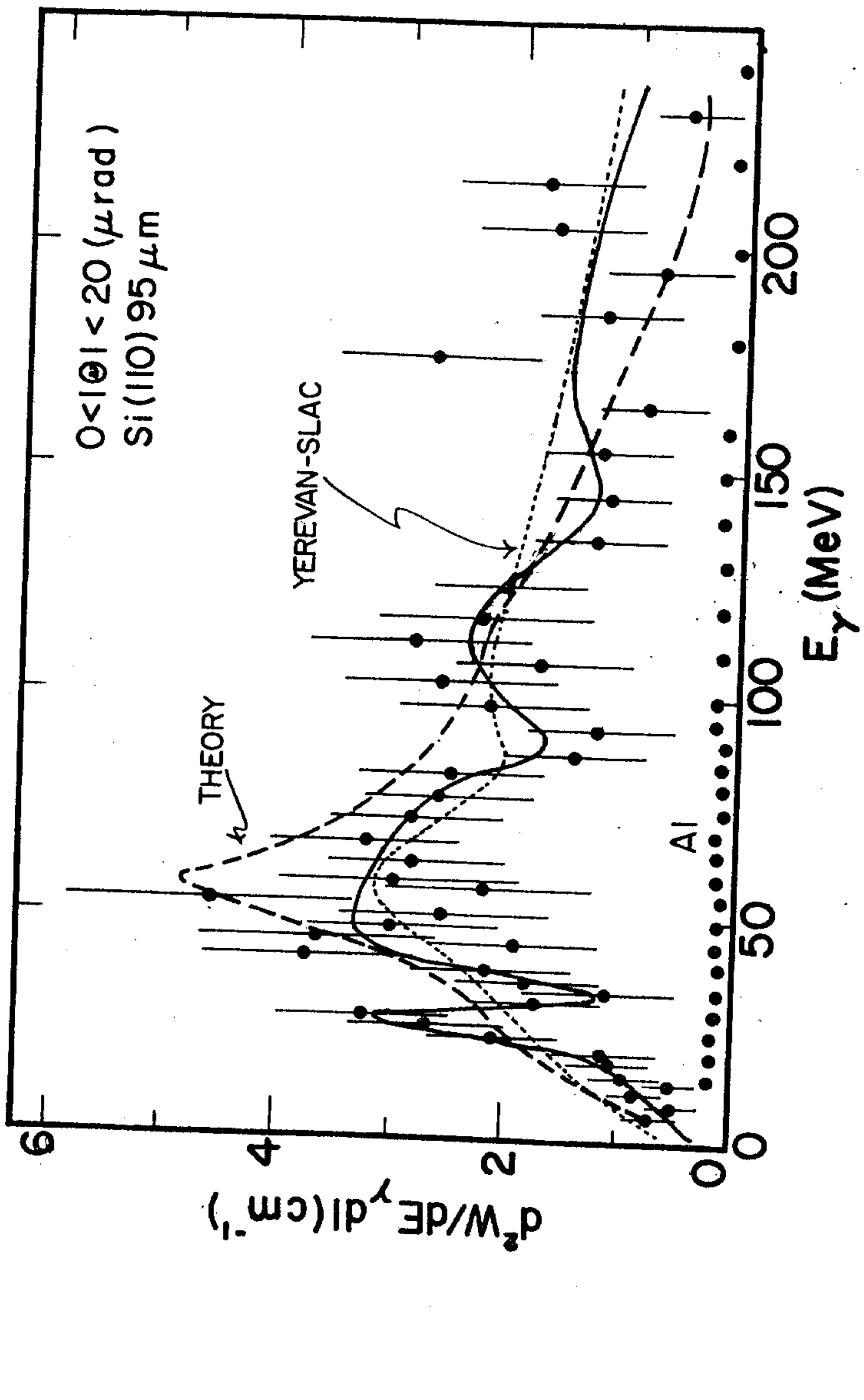
0<|Θ|<20 (μrad)
Si (110) 95 μm
THEORY
YEREVAN-SLAC
Al
0
50
100
150
200
E_γ (MeV)
0
2
4
6
d²W/dE_γdl (cm⁻¹)

Fig. 2

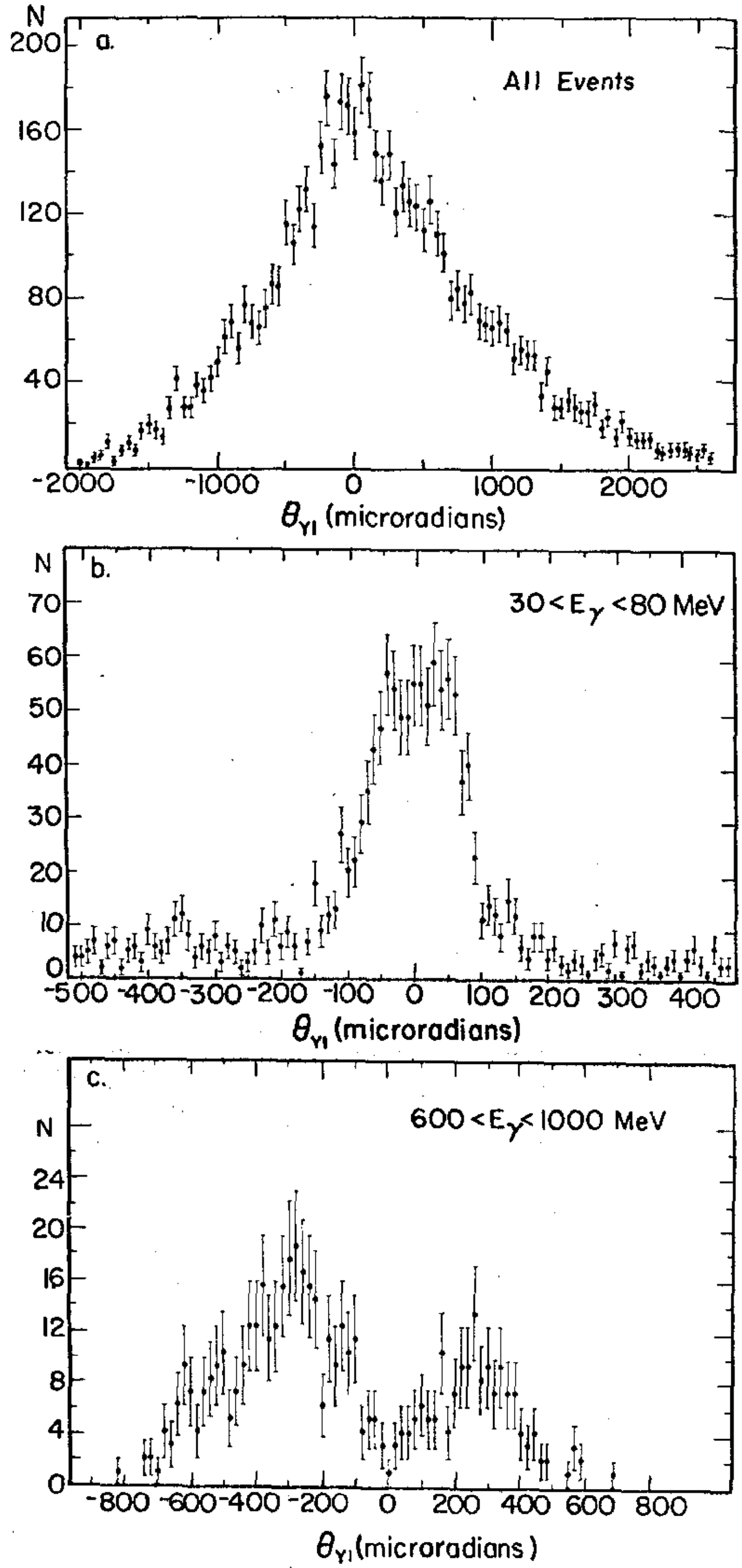

N
200
160
120
80
40
a.
All Events
-2000
-1000
0
1000
2000
θ_{Y1} (microradians)
N
70
60
50
40
30
20
10
0
b.
30 < E_γ < 80 MeV
-500 -400 -300 -200 -100 0 100 200 300 400
θ_{Y1} (microradians)
c.
600 < E_γ < 1000 MeV
N
24
20
16
12
8
4
0
-800 -600 -400 -200 0 200 400 600 800
θ_{Y1} (microradians)

Fig. 3

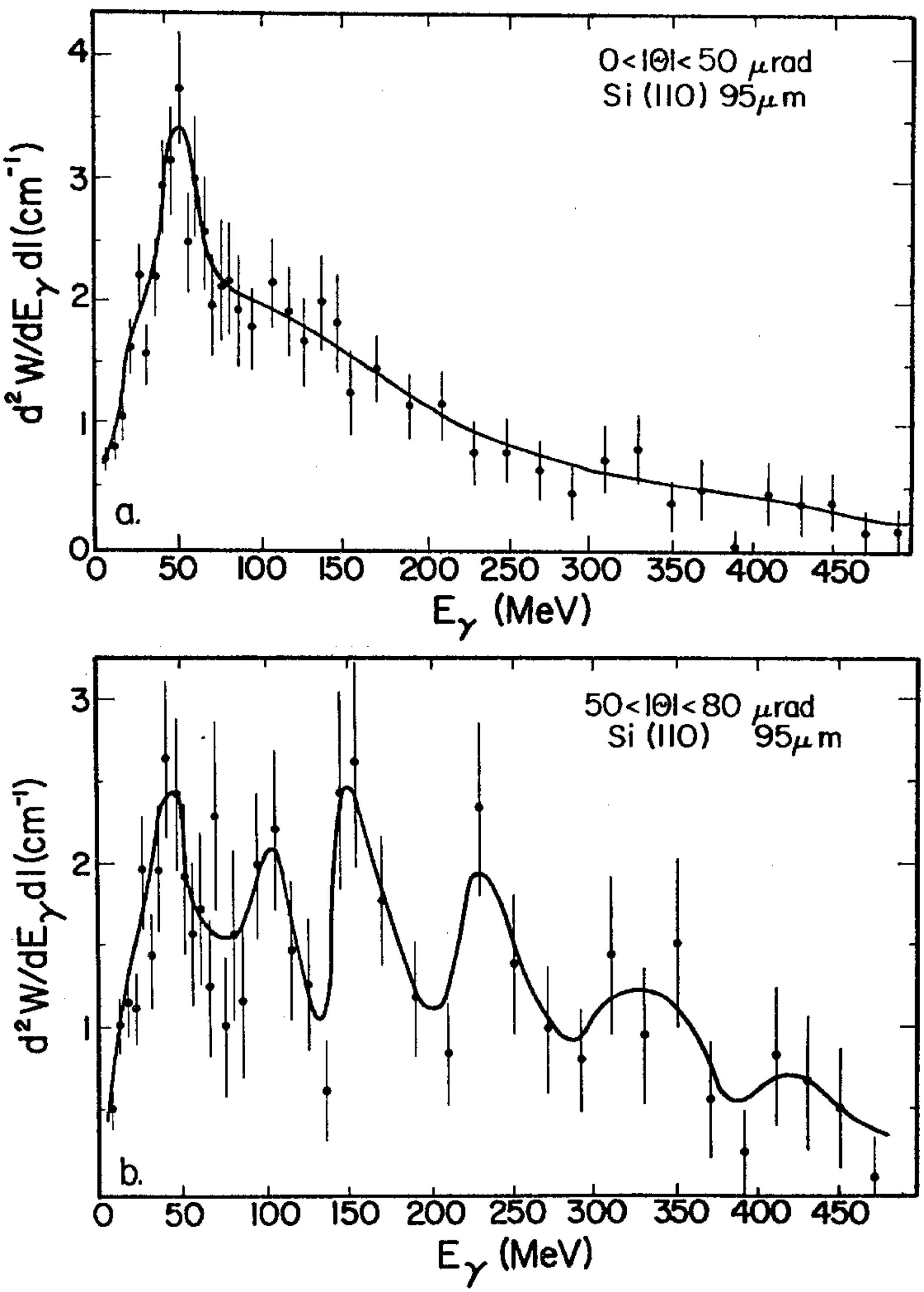
0<|Θ|<50 μrad
Si (110) 95μm
a.
d²W/dEγdl(cm⁻¹)
Eγ (MeV)
50<|Θ|<80 μrad
Si (110) 95μm
b.
d²W/dEγdl(cm⁻¹)
Eγ (MeV)

Fig. 4